

PRIMARY RESEARCH

Open Access



miR-145 supports cancer cell survival and shows association with DDR genes, methylation pattern, and epithelial to mesenchymal transition

Siddharth Manvati¹, Kailash Chandra Mangalhar², Ponnuswamy Kalaiarasan¹, Rupali Chopra², Gaurav Agarwal³, Rakesh Kumar⁴, Sunil Kumar Saini¹, Monika Kaushik¹, Ankita Arora¹, Usha Kumari⁵, Rameshwar Nath Koul Bamezal² and Pawan Kumar Dhar^{1*}

Abstract

Background: Despite several reports describing the dual role of miR-145 as an oncogene and a tumor suppressor in cancer, not much has been resolved and understood.

Method: In this study, the potential targets of miR-145 were identified bio-informatically using different target prediction tools. The identified target genes were validated in vitro by dual luciferase assay. Wound healing and soft agar colony assay assessed cell proliferation and migration. miR-145 expression level was measured quantitatively by RT-PCR at different stages of breast tumor. Western blot was used to verify the role of miR-145 in EMT transition using key marker proteins.

Result: Wound healing and soft agar colony assays, using miR-145 over-expressing stably transfected MCF7 cells, unraveled its role as a pro-proliferation candidate in cancerous cells. The association between miR-145 over-expression and differential methylation patterns in representative target genes (*DR5*, *BCL2*, *TP53*, *RNF8*, *TIP60*, *CHK2*, and *DCR2*) supported the inference drawn. These in vitro observations were validated in a representative set of nodal positive tumors of stage 3 and 4 depicting higher miR-145 expression as compared to early stages. Further, the role of miR-145 in epithelial–mesenchymal (EMT) transition found support through the observation of two key markers, Vimentin and *ALDL*, where a positive correlation with Vimentin protein and a negative correlation with *ALDL* mRNA expression were observed.

Conclusion: Our results demonstrate miR-145 as a pro-cancerous candidate, evident from the phenotypes of aggressive cellular proliferation, epithelial to mesenchymal transition, hypermethylation of CpG sites in DDR and apoptotic genes and upregulation of miR-145 in later stages of tumor tissues.

Keywords: miR-145, SMAD3, BRCA2, DR5, Epithelial–mesenchymal transition, Vimentin, Methylation

Background

MicroRNAs are small non-coding RNA molecules with a potential to regulate the cellular machinery directly or indirectly. Functions of most of the ~1900 mature miRNA identified till date remain to be understood

properly. miR-145 is one such candidate reported to play a dual role, of a tumor suppressor by targeting the expression of, *FLI1* [1, 2], *TIRIP* [3], *SOX9* [4], *VEGF* [5], *Ets 1* [6], *YES*, *STAT1* [7], *p70S6K1* [8], *Dab2* [9], *PAK4* [10], *JAM-A* [11], *CLDN10* [12] *FSCN1* [13], *RTKN* [14] genes; and in the neointimal formation of vascular smooth muscle cells [15]. miR-145 has also been reported to facilitate ES cell differentiation by repressing the core pluripotency factor, *OCT4* [16].

*Correspondence: pawandhar@mail.jnu.ac.in

¹ School of Biotechnology, Jawaharlal Nehru University, New Delhi, India
Full list of author information is available at the end of the article



The expression of miR-145 has been reported to be down-regulated in cervical [17], hepatic [18] and hepatocellular [19], colorectal [20, 21], serous ovarian [22], ovarian [23], colon [24], oral [25], prostate [26], gastric [27], bladder [28], nasopharyngeal [29], lung [30], ACTH-secreting pituitary [31], B-CLL (B cell chronic lymphocytic leukemia) [32] and breast [33] cancers, dedifferentiated VSMCs and balloon-injured arteries [34], acute and chronic vascular stress [35], myelodysplastic syndrome [36]. Whereas, in pancreatic ductal adenocarcinoma [32], polycythemia vera [37], multiple sclerosis [38], the expression of miR-145 was found to be up-regulated. Suggestions of miR-145 playing a role in the development of colon and rectal cancers but not in its progression [39] have been made, thus raising a question about its exact role in tumour initiation and development. It was, therefore, pertinent to understand the dual role of miR-145 in cancer, using both in vitro and cellular assays.

Results

miR-145 down-regulates mRNA expression of SMAD3, DR5, BRCA2

The targets of miR-145 were predicted using bio-informatics tools. Of 19,980 predicted 3'UTR targets (PicTar: 196; mirDB: 542; miRanda: 19,242), 58 emerged common amongst all the three tools used (Fig. 1a), showing SMAD3, DR5, BRCA2 with highest prediction scores. Validation of the presence of miR-145 binding site at 3'UTR (Fig. 1b) in the three targets using luciferase reporter assay, showed a significantly decreased activity in presence of exogenous miR-145 in MCF7 (SMAD3: 0.51; DR5: 1.23; BRCA2:0.30) and HepG2 (SMAD3:0.51; DR5: 1.23; BRCA2: 0.30) cells, when compared with the activity of luciferase reporter without miR binding site (MCF7: 4.38; HepG2: 5.08) (Fig. 1c).

Further validation of the three targets, through their cellular status in MCF7 cells with over-expressing miR-145, exhibited decreased expression of SMAD3; DR5; BRCA2 (0.04-fold; 0.1-fold; 0.6-fold) when compared to the control (pEP-miR-Mock considered as onefold). Inhibition with anti-miR-145, resulting in a reversal and an increased expression in cells of the three target genes (1.5-fold; 1.7-fold; 1.9-fold) as compared to mock control (anti-miR-mock considered as onefold) confirmed that miR-145 targeted these three targets (Fig. 1d). The protein expression of one of the novel targets SMAD3, performed using Western Blotting was observed to be downregulated in presence of miR-145 precursors as compared to control mimics (Fig. 1e).

miR-145 over-expression in late stage tumour tissues correlates with apoptotic and DDR gene methylation in vitro

In-vivo studies in a representative set of 72 (36 pairs) samples showed down-regulated expression of miR-145 in sporadic breast tumours when compared to adjoining normal tissue (Fig. 2a). However, the stage wise analysis revealed that the expression of miR-145 increased significantly in tumour samples grouped together for stage 3+stage 4 as compared to tumour samples belonging to stage 1+stage 2 (Fig. 2b). Interestingly, miR-145 expression showed an increase with the number of nodes involved (Fig. 2c) with a concomitant differential methylation pattern of most of the studied CpG positions in apoptotic and DDR genes (*DR5*, *BCL2*, *TP53*, *RNF8*, *TIP60*, *CHK2*, *DCR2*), both in vivo and in vitro experiments (Additional file 1: Table S1).

The methylation status of CpG positions of genes related to cell death and survival [40] was assessed in vitro in miR-145 stably transfected and over-expressing MCF-7 cells and validated in vivo in a representative set of sporadic breast cancer tissues (Figs. 3, 4; Additional file 1: Table S1). The methylation status of DR5 CpG positions (−93, −91) revealed increased average percentage methylation (stage 1+2: 2%; stage 3+4: 2.88%) in tumors, correlating with the observations made in vitro. Further, DR5 methylation at CpG position (−93, −91) showed an increased methylation with the number of nodes involved (N0: 1.00%; N1: 1.5%; N2: 2.00%; N3: 5.00%), supporting what was observed in in vitro between DR5 methylation/regulation and experiments with miR-145 over-expression. A simultaneous hypermethylation of *BCL2*, *TP53*, *RNF8* and hypomethylation of *DCR2*, *CHK2* observed in vitro and in vivo studies supported the assessment of pro-proliferative role of miR-145.

Since a positive association between DNA damage response with epithelial to mesenchymal transition [41] and induction of methylation [40] has been reported, it was pertinent to adjudge our conclusions on EMT by confirming the association of miR-145, if any, with chosen DDR genes both in miR-145 over-expressing MCF-7 cells and in sporadic breast cancer tissues.

miR-145 over-expression supports aggressive proliferation and epithelial to mesenchymal transition (EMT)

The wound healing assay using MCF7 cells showed that the average migration in: (i) untransfected cells—109 ± 10 mm (pre-wounding: 314 ± 10 mm; post-wounding: 205 ± 10 mm); (ii) pEP-miR-Mock cells—161 ± 20 mm (pre-wounding: 424 ± 20 mm; post-wounding: 263 ± 21 mm); and (iii) pEP-miR-145 transfected cells—302 mm ± 15 mm (pre-wounding:

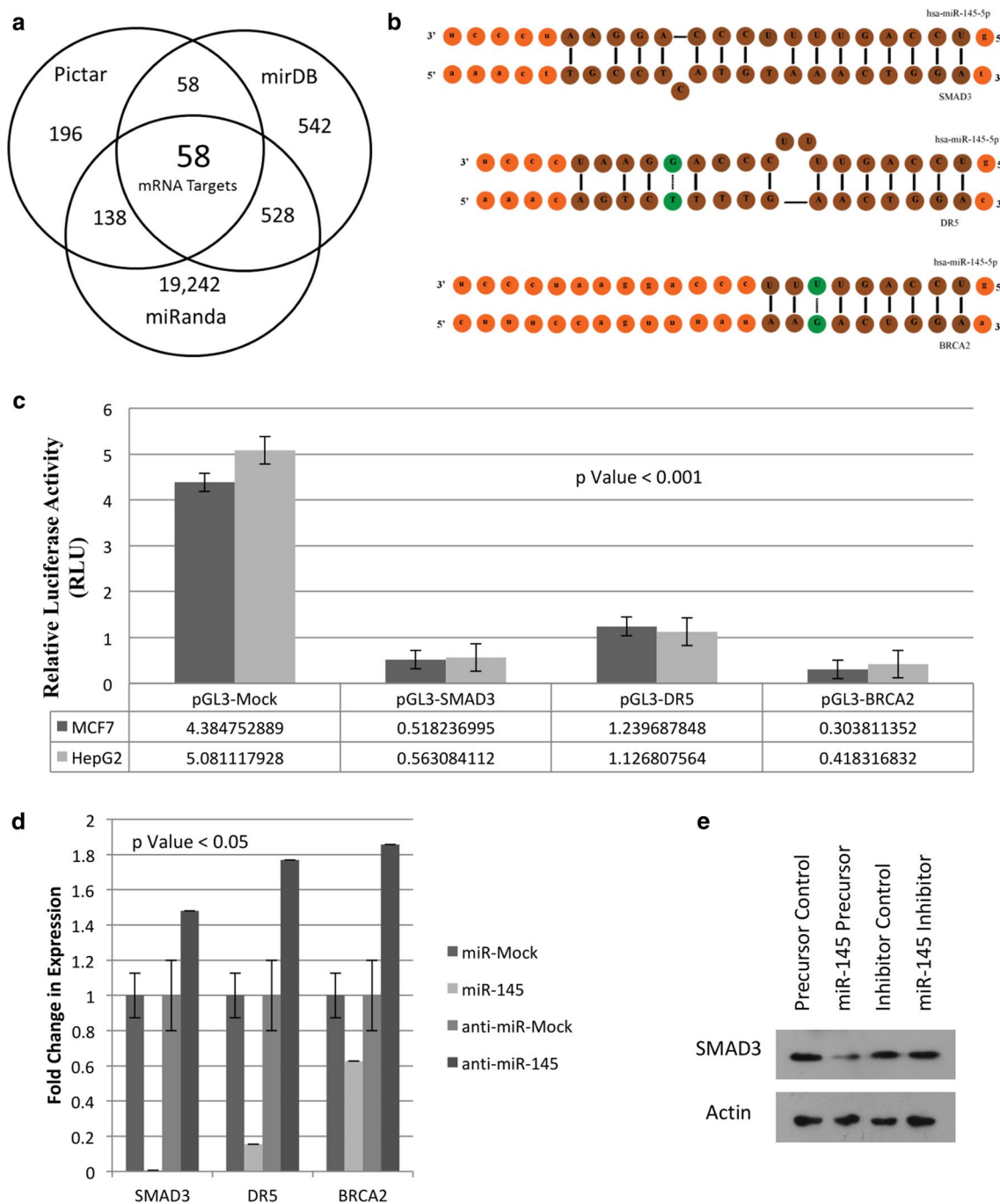
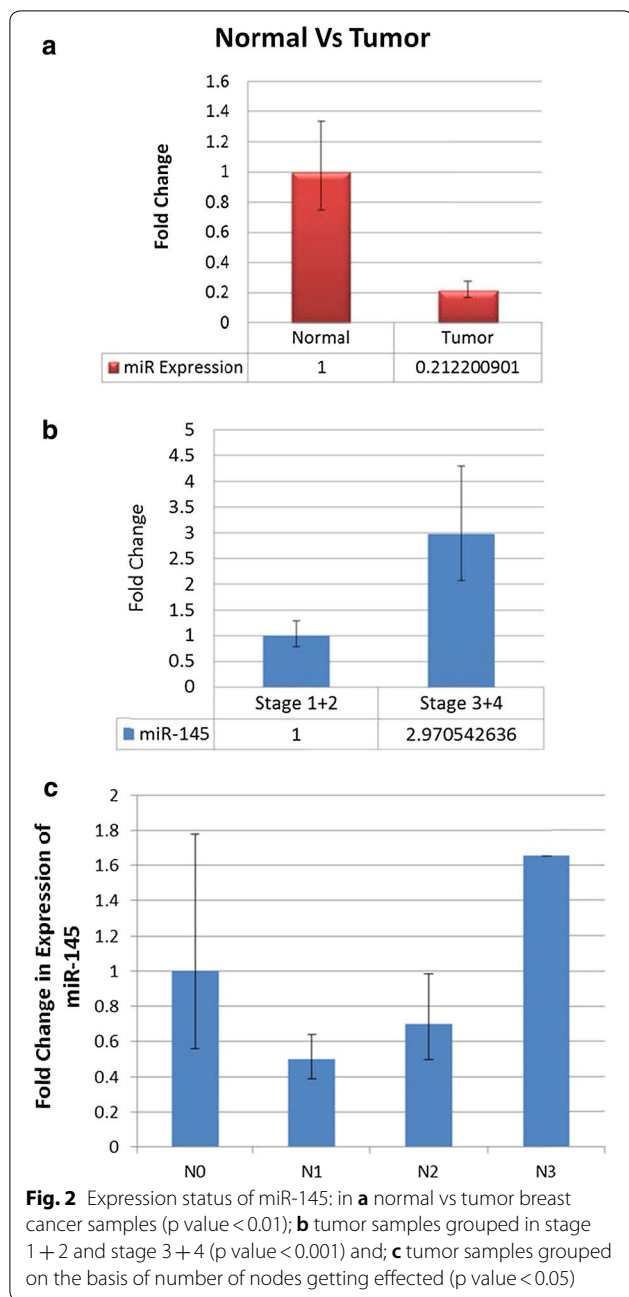


Fig. 1 SMAD3, DR5 and BRCA2 as the novel targets of miR-145: **a** Predicted 58 common targets for miR-145 in all the three tools (PicTar, mirDB and miRanda), which included SMAD3, DR5 and BRCA2 with highest score; **b** binding sites of miR-145 identified at the 3'UTR region of the three targets, SMAD3, DR5 and BRCA2; **c** *Luc* gene activity showing a significant decrease when miR-145 was over-expressed in cells expressing *Luc* with 3'UTR of SMAD3 or DR5 or BRCA2, in MCF7 and HepG2 cells; **d** real-time PCR using Sybergreen, showing a significant decrease and increase in fold change of mRNA expression of identified targets (SMAD3, DR5 and BRCA2) in MCF7 cells under miR-145 and anti-miR-145 transfected conditions, respectively. **e** Western blotting of SMAD3 in presence and absence of miR-145 in MDAMB231 cell line



449 ± 17 mm; post-wounding: 147 ± 19 mm) (Fig. 5a), supported cellular migration due to miR-145 over-expression. Further, the number of colonies in soft agar when counted under each condition, showed on an average: only 1 ± 1 colony in un-transfected MCF7 cells, 2 ± 1 colonies in pEP-miR-Mock cells and 11 ± 2 colonies in pEP-miR-145 cells (Fig. 5b). These findings supported the role of miR-145 over-expressing cells in acquiring an apparent anchorage independent growth potential. The miR-145 over-expressing cells, when assessed for the status of EMT markers-Vimentin and *ALDL*, showed a

direct correlation. Vimentin expression increased with miR-145 up-regulation, and decreased upon down-regulation of miR-145 (Fig. 5c). Real-time PCR analysis of the expression of *ALDL* showed a decrease (0.2-fold) and increase (sixfold) in presence and absence of miR-145 (Fig. 5d), respectively, as compared to mock (pEP-miR-Mock and anti-miR-Mock considered as onefold, respectively). Such a profile specific to EMT was suggestive of the involvement of miR-145 in epithelial to mesenchymal transition.

Discussion

The targets of miR-145 identified bio-informatically and validated in cellular assays using both precursor and anti-miR-molecules belonged to different cellular pathways. The commonest feature that emerged in the path-way biology between the three targets, SMAD3, DR5, BRCA2, was of regulation of cellular proliferation despite genomic instability.

It was obvious that down-regulation of the two targets, SMAD3 and DR5, which are known to inactivate TGF-β, inhibiting apoptotic pathway [41] and compromising extrinsic apoptotic induction [44], would result in anti-apoptotic state of the cells, supporting cell survival. Whereas, BRCA2, involved in maintaining genomic stability of the cells [42], when down-regulated with miR-145, was expected to result in accumulation of DNA damage [43]. Anti-apoptosis taken together with DNA damage has been reported to create genomic instability [44] which leads to uncontrolled cellular proliferation like characteristics [45], with a potential role in cancer. This role of miR-145 in facilitating cell proliferation and survival, as observed in wound healing assay and the features associated with epithelial–mesenchymal transition (EMT) (Fig. 5), found support in the epigenetic study of a select set of apoptotic and DDR genes in a representative set of sporadic breast tumours (Figs. 3, 4). Here, in stage 3 and 4 tumours, not only was the expression of miR-145 high (Fig. 2) but it showed similar features of induction of epigenetic imprint in the studied genes, as was observed in miR-145 over-expressing cells in vitro (Figs. 3, 4). These findings along with the bio-informatics pathway analysis, identifying cross talk with molecules involved in growth and EMT (Additional file 2: Figure S1), supported that regulation of SMAD3, DR5 and BRCA2 by miR-145 plays a significant role in uncontrolled cellular proliferation with relevance in cancer.

Earlier studies have reported that metastasis/cellular aggressiveness are accompanied with epithelial to mesenchymal transitions [46]; and the EMT was found to be induced by damaged DNA [47]. Keeping these reports and our observations in view, the epigenetic status of genes involved in survival (anti-apoptotic)

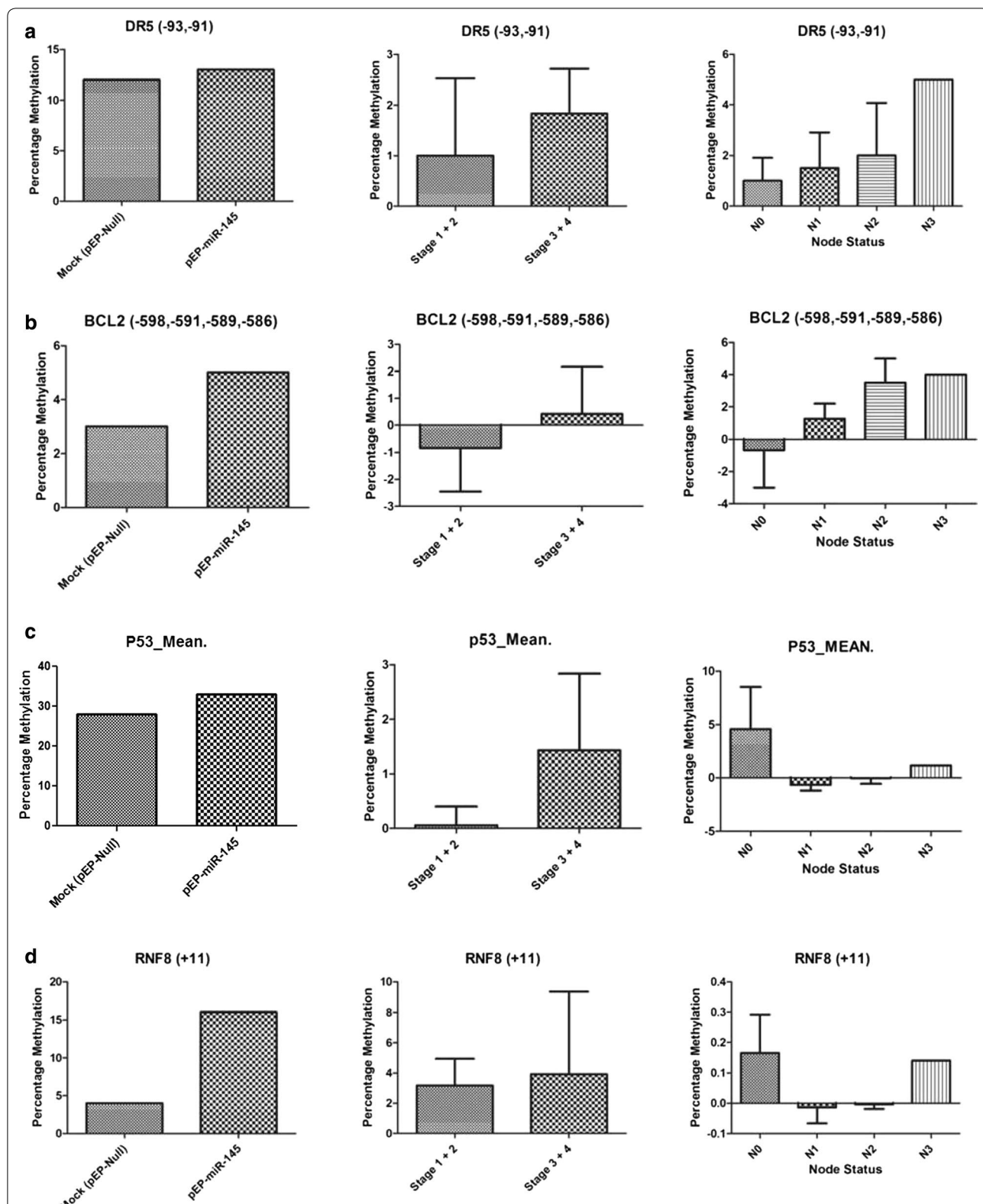
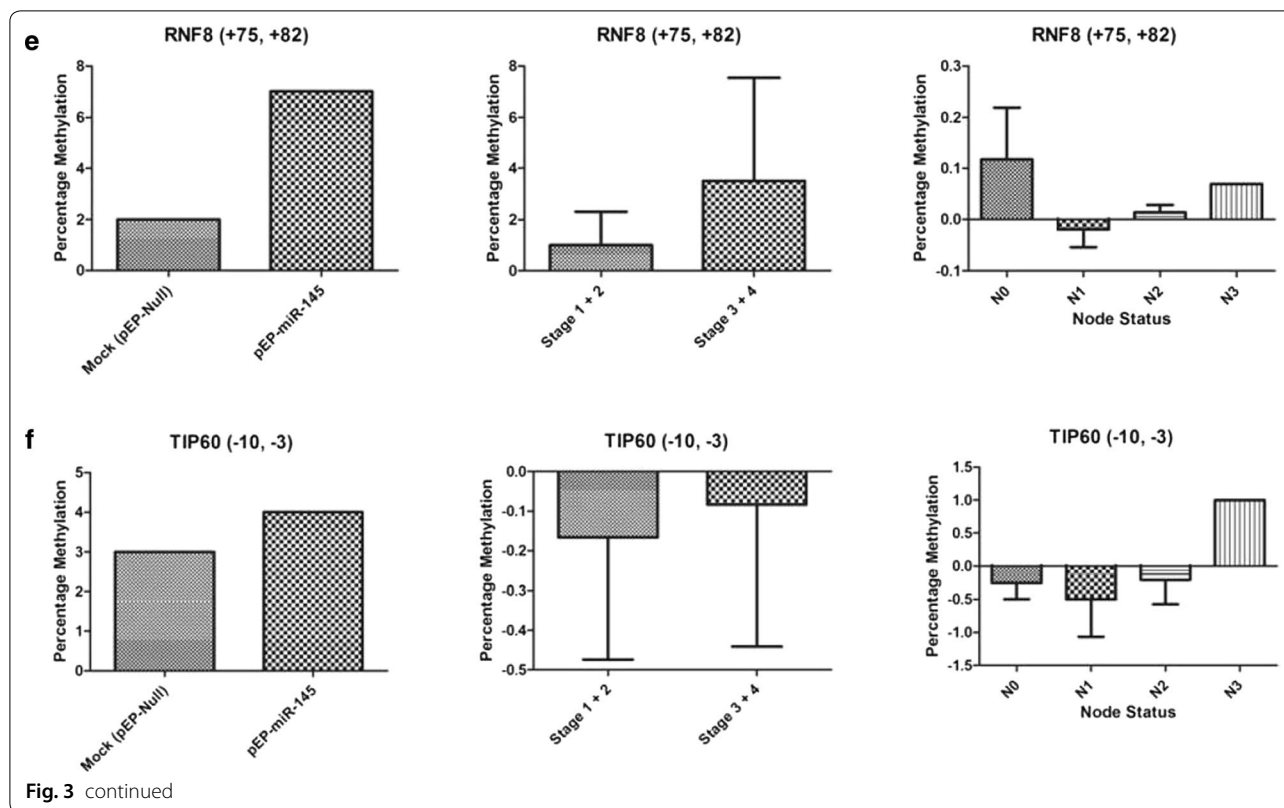


Fig. 3 Increasing methylation pattern: observed at different CpG positions within the gene **a** *DR5* (− 93, − 91), **b** *BCL2* (− 598, − 591, − 589, − 586), **c** *TP53* (− 78, − 75, − 22, − 15, + 91, + 158, + 171, + 175), **d** *RNF8* (+ 11), **e** *RNF8* (+ 75, + 82) and **f** *TIP60* (− 10, − 3) when compared in miR-145 over-expressing stable cells, tumor stage wise groups and node status of breast cancer samples



and death (apoptotic) pathway was analysed in tumour samples studied earlier [40] and under in vitro miR-145 regulation in the present study. No significant change in expression as well as methylation pattern of CpG positions of death inducing (70 positions) and survival genes (59 positions) was observed in tumour samples (Data not shown) as well as miR-145 expressing (pEP-miR-145) stable cells as compared to mock (pEP-miR-Mock) controls. Similarly, no difference in cellular viability, measured using MTT assay was observed in these cells as well (Additional file 2: Figure S2). However out of 139 CpG positions studied, the average percentage methylation (Additional file 1: Table S1) of only CpG positions of *BCL2*, *TP53*, *RNF8*, *TIP60*, *CHK2*, *DCR2* (Figs. 3, 4) showed association with expression status of miR-145. We were able to observe 6 CpG positions where methylation increased (Fig. 3) and 4 CpG positions where methylation decreased (Fig. 4), under the influence of increased expression of miR-145, both in vivo (tumours) and in vitro conditions. Such hyper (*DR5*, *BCL2*, *TP53*, *RNF8*) and hypo (*CHK2*, *DCR2*) methylation supported the observation of miR-145 being pro-proliferative in nature. These positions were subjected to in silico transcription factor analysis (Using Alibaba 2.2). It was observed that methylation in *DR5* was able to create RAP1 binding site, where

an elevated RAP1 is known to regulate the activity of E-Cadherin [48], a hallmark for EMT [49]. An overall methylation in *TP53* resulted in the creation of a new binding site for OCT-1. Accumulation in OCT-1 has also been associated with unregulated EMT [50–52]. These observations have added strength to our findings of association of miR-145 with EMT pathway. To sum up, we identified *SMAD3*, *DR5* and *BRCA2* as novel targets for miR-145. Apart from *DR5*–3'UTR being the target of miR, we also identified the increase in methylation of *DR5*, *BCL2*, *TP53*, *RNF8* and concomitant hypo methylation in *DCR2*, and *CHK2* promoter regions in presence of miR-145.

Conclusion

In conclusion, our study identified *SMAD3*, *BRCA2* and *DR5* as novel targets of miR-145 and observed the epigenetic association between the increased expression of microRNA and the differential epigenetic regulation of apoptotic and DDR gene related cellular machinery. Keeping in view the observations made, both in vivo and in vitro, we conclude that miR-145 has a pro-proliferative role in late stage node positive tumours and in regulating EMT transition. The association between miR-145 over-expression and differential methylation patterns in in vitro studies and stage 3+4 node positive tumours in

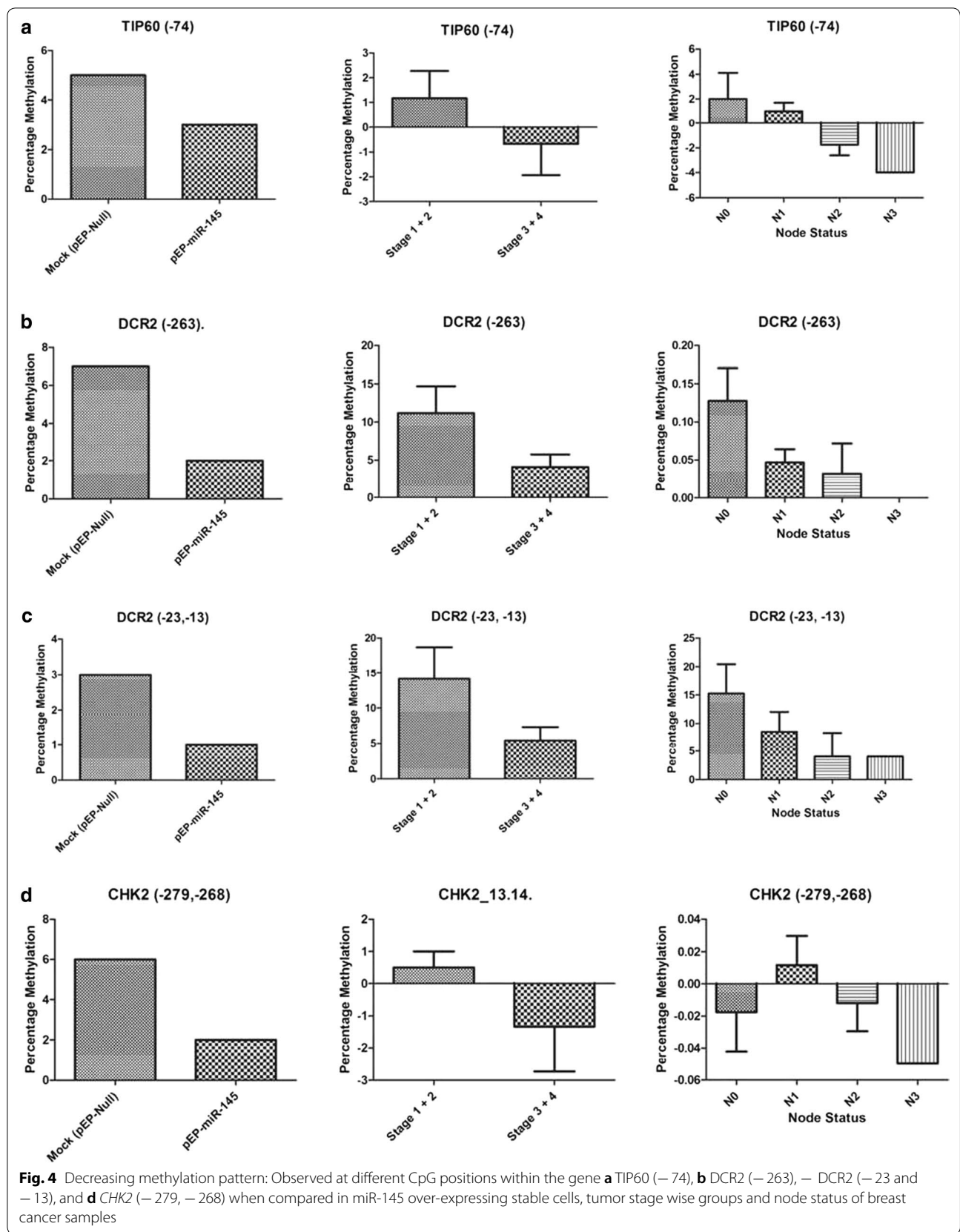


Fig. 4 Decreasing methylation pattern: Observed at different CpG positions within the gene **a** TIP60 (– 74), **b** DCR2 (– 263), – DCR2 (– 23 – 13), and **d** CHK2 (– 279, – 268) when compared in miR-145 over-expressing stable cells, tumor stage wise groups and node status of breast cancer samples

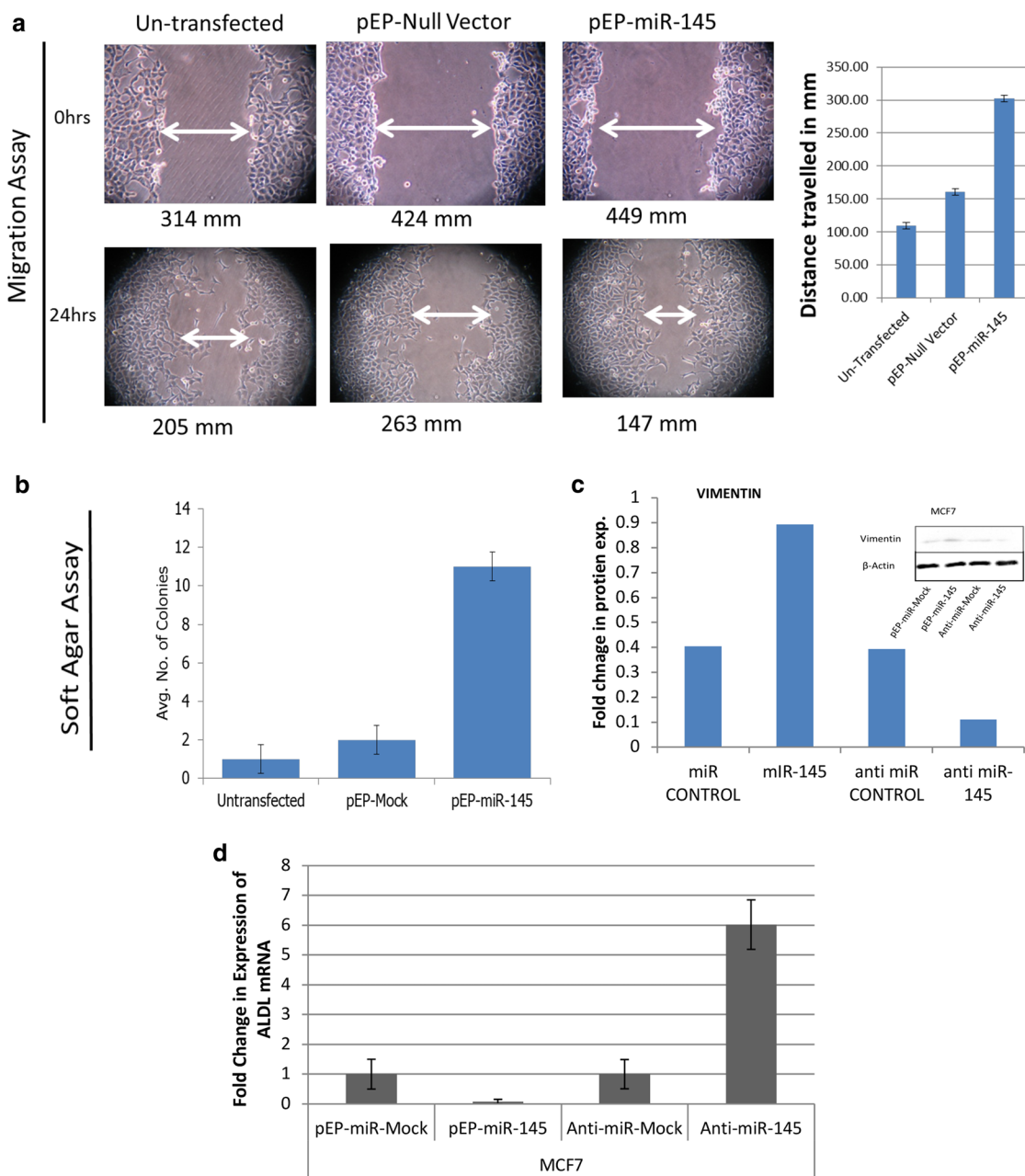


Fig. 5 miR-145 over-expression enhanced migration and supported EMT: MCF7 cells (untransfected, pEP-miR-Mock stable and pEP-miR-145 stable) **(a)** were seeded in 6-well plates. 24 h after seeding, a cell free zone was created using sterilized pipette tip and this was defined as 0 h (pre-wounding). Cellular migration in the cell free zone was visualized in pre-wounding wells (0 h) and post-wounding wells (after 24 h). The images were analysed using ImageJ and the distance between two walls of cell free zone (post-wounding–pre-wounding) of miR-145 over-expressing stable cells were found to be significantly decreased as compared to mock transfected stable cells; **b** cells cultured in soft agar and on 14th day fixed and stained using coomassie blue. The miR-145 over-expressing stable cells formed defined colonies suggesting their role in colony formation; **c** Western blots of Vimentin over-expression and down-regulation, and real-time PCR of ALDL mRNA down-regulation and over-expression upon miR-145 over-expression and inhibition, respectively, supporting the positive influence of miR-145 on EMT, in MCF7 cells

the representative target genes (*DR5*, *BCL2*, *TP53*, *RNF8*, *TIP60*, *CHK2*, and *DCR2*) supports these inferences.

Materials and methods

Bio-informatics predictions

The targets for miR-45 were predicted using three target prediction program (miRanda 3.3a [53], TargetScan 6.2 [54] and RNAhybrid 2.1 [55]). Fasta sequence of hsa-miR-145 was retrieved from miRBase. The binding site in the predicted targets for miR-145 was scanned using default parameters in all three software's. 3'UTR sequences of SMAD3, BRCA2 and DR5 genes were retrieved from UCSC genome table browser.

Cloning

miR-145 expressing vectors were generated using pre-miR amplicon of miR-145 from genomic DNA and pEP-miR vector (Cell Biolabs) as backbone. The pre-miR sequence was obtained using primer sets (Additional file 3: Table S2) and amplified from human genomic DNA by simple PCR reaction. The primers (IDT) were designed using online (Primer 3) and offline (Oligo) tools such that the 5' ends of each forward and reverse primer contained *Nhe*-I and *Bam*HI restriction sites, respectively. These sites were also identified in pEP-miR vector for cloning purposes. After amplification the product was digested and cloned into pEP-miR vector, generating pEP-miR-145 recombinant clone. For anti-miR conditions; commercially available controls and inhibitor molecules were purchased (Applied Biosystems) and used.

Luciferase assay

The 3'UTR of novel targets, established bio-informati-cally, were cloned into the 3'UTR of pGL3-Control vector (Promega) at *Xba*-I site. The 3'UTR was amplified from human genomic DNA, using primer (IDT) sets (Additional file 3: Table S2). The amplicons were then cloned, generating pGL3-SMAD3, pGL3-BRCA2 and pGL3-DR5 vectors. All the clones were verified for containing the desired insert, by colony PCR, restriction digestion and DNA sequencing. Both pGL3 control and pEP-miR-145 (The miR-145 expressing vector) constructs were co-transfected in two different cell lines, MCF7 and HepG2. The transfection was performed using ESCORTS (Sigma-Aldrich) reagent and according to manufacturer's protocol. The assay was performed after seeding in MCF7 and HepG2 cells, in a 24-well plate, using Dual-Luciferase Assay Kit (Promega). After 48 h of transfection the cells were measured for Firefly and Renilla luminescence, using luminometer. The ratio of Firefly and Renilla reporter in presence of pEP-miR-145 was calculated and used in defining the change in expression of Firefly reporter in co-presence of predicted binding sites of specific genes.

Wound-healing assay

To begin with the untransfected, pEP-miR-Mock and pEP-miR-145 transfected cells were seeded in 6-well plates. A cell free zone was created, 24 h after seeding, using a pipette tip. This was termed as pre-wounding well (0 h). These cells were allowed to grow for 24 h (post-wounding). These cells were visualized and images were captured. The images were analysed using ImageJ software and the distance between the cellular walls of pre-migration and post-migration were measured.

Generation of stable cells

pEP-miR-145 and pEP-Mock (Vector containing Anti-puromycin gene) were transfected independently in MCF7 cells using ESCORT (Sigma-Aldrich) reagent. The transfected cells were grown in media containing puromycin as selection marker. After seven passages the cells were verified for transient expression of miR-145 before further experimentation was performed. Thereafter, these sets of miR-145 expressing and pEP-mock transfected cells were cultured in puromycin containing media for all experimentation.

Soft-Agar assay

miR-145 expressing and pEP-Mock stable cells were re-suspended in 2-ml 0.3% agar medium. Each embedded cell mixture was overlaid on 1.5 ml, 0.6% agar in 6-well plates, and a 1.5-ml top layer of 0.6% agar added to each well to prevent evaporation. The cultures were incubated in a humidified incubator at 37 °C and 5% CO₂ for about 2 weeks. Cell colonies were stained with giemsa and counted using a conventional microscope [56].

Western blotting

Cell lysate were prepared by incubating cells in buffer containing 0.5% sodium deoxycholate, 1% Triton X-100, 50 mM Tris pH 7.2, 150 mM NaCl, 10% glycerol, 0.1% SDS, 1 mM dithiothreitol (DTT), 1 mM sodium vanadate (NaV), 1 mM phenylmethylsulfonyl fluoride (PMSF), 5 mM sodium fluoride (NaF), phosphatase inhibitor cocktail (Sigma), 4 µg/ml each of pepstatin, aprotinin and leupeptin (Sigma), on ice for 30 min. Concentration of isolated protein was estimated using Pierce BCA (bicinchoninic acid) protein assays as per the manufacturer protocol. Separation of proteins was done on 10% SDS-PAGE, later transferred to nitrocellulose membrane (mci) overnight at 4 °C (wet transfer), and probed with primary antibodies. Membrane was incubated with appropriate secondary antibody for 1 h at room temperature. Proteins were detected using enhanced chemiluminescence kit from Thermo Scientific, USA. Primary antibodies used were: anti-vimentin and anti-β-actin (Cell signaling Technology).

Real-time PCR

Total RNA was extracted using traditional TRIzol (Sigma) method. RNA quality was analyzed by electrophoresis on 1.2% agarose formaldehyde gel and quantified by A260/A280 absorbance equilibrium. 1–2 µg of total RNA was reverse transcribed into single stranded DNA using High-Throughput cDNA preparation kit (Applied Biosystems). Sybr-Green assay (Applied Biosystems) was used for quantitating mRNA levels of ALDL. GAPDH was used as endogenous control. Real time PCR was carried out on ABI Prism 7000 Sequence Detection System (Applied Biosystem). $\Delta\Delta C_t$ (Cycle threshold) method of relative quantification was used to calculate fold change in gene expression by SDS 1.1 RQ software (Applied Biosystems).

Methylation analysis

CpG positions (nomenclature as per transcription start site (TSS)) of apoptosis and DDR pathway genes were selected and identified as per earlier study [40]. The EZ-96 DNA Methylation Kit (Zymo Research) was used for bisulfite conversion of the target sequences. PCR products were analyzed further in Sequenom MassARRAY.

Statistical analysis

Spearman's correlation coefficient and Fisher's exact test was calculated using the SPSS version 13. *p* value at and below ≤ 0.05 was considered significant.

Supplementary information

Supplementary information accompanies this paper at <https://doi.org/10.1186/s12935-019-0933-8>.

Additional file 1: Table S1. Percentage methylation values of 10 CpG positions: identified to be up regulated or down regulated in association with miR-145 expression under both in-vitro (Mock, miR-145) and in-vivo (Stage 1 + 2, Stage 3 + 4, Node 0, Node 1, Node 2, Node 3) and conditions.

Additional file 2: Figure S1. Bio-informatics prediction of cross-talk between miR-145, SMAD3, BRCA2 and DR5. **Figure S2.** miR-145 constrains mRNA expression of death inducing genes: Comparison of (a) the average pooled mRNA expression, by Real-Time PCR, of death inducing (BRCA2, CYC, DR5, MDM2, ALDL, SMAD3, TGFB) Vs survival inducing (FLIPL, BCL2, CASP8L, TP53, PKM2) genes suggests constrained expression of death inducing genes under miR-145 up-regulation as compared to miR-145 inhibition. (b) the average percentage methylation of CpG positions of death inducing genes (70 positions) and survival inducing genes (59 positions), and (c) the cellular viability, under pEP-miR-Mock and exogenous pEP-miR-145 overexpression, suggested no significant change.

Additional file 3: Table S2. List of primers used for cloning.

Abbreviations

EMT: epithelial to mesenchymal transition; MiR: microRNA; DDR: DNA damage response; 3' UTR: 3' untranslated region; PMSF: phenylmethylsulfonyl fluoride.

Acknowledgements

Authors wish to acknowledge the support provided by Prof Rajiv Bhat (School of Biotechnology, Jawaharlal Nehru University, New Delhi, INDIA) and Dr. Niloo Srivastava (Scientist 'D', Department of Biotechnology, Govt. of India). SM acknowledges fellowship support provided by DSKPDF-UGC. PKD acknowledges support provided by JNU-UGC-UPE-II, DBT, DST, CSIR and ICMR.

Authors' contributions

SM participated in the study design, performed major laboratory work and statistical analyses and wrote the manuscript; KM helped in performing luciferase assay and provided critical comments for the manuscript; PK performed the bioinformatics analysis for the study. RC performed methylation assay on SEQUENOM MassARRAY platform. GA provided the tissue samples and the clinical profile of the patients with sporadic breast cancer. RK, MK and SK assisted in manuscript preparation. RNKB and PKD participated in the study design, facilitated the execution of the study and provided the critical revision of the manuscript. All authors read and approved the final manuscript.

Funding

Authors acknowledge SMVDU, JNU-UPE-II, DST, DBT and UGC India for providing necessary funds to execute the related experiments. SM acknowledges fellowship support from UGC-DSKPDF.

Availability of data and materials

The material and data defined in the manuscript is available on demand by contacting the corresponding author at pawandhar@mail.jnu.ac.in.

Ethics approval and consent to participate

The manuscript contains data of human tissue procured from Dr. Gaurav Agarwal, Sanjay Gandhi Postgraduate Institute of Medical Sciences, Lucknow, Uttar Pradesh, India, after internal ethical approval and prior patient consent for publication. The samples were processed at Jawaharlal Nehru University for experimental purposes.

Consent for publication

All authors have read the manuscript and provided their consent for publication.

Competing interests

The authors declare that they have no competing interests.

Author details

¹ School of Biotechnology, Jawaharlal Nehru University, New Delhi, India. ² National Centre of Applied Human Genetics, School of Life Sciences, Jawaharlal Nehru University, New Delhi, India. ³ Sanjay Gandhi Postgraduate Institute of Medical Sciences, Lucknow, Uttar Pradesh, India. ⁴ School of Biotechnology, Shri Mata Vaishno Devi University, Kakryal, Katra, Jammu and Kashmir, India. ⁵ Faculty of Medicine, AIMST University, Bedong, Malaysia.

Received: 3 August 2018 Accepted: 18 August 2019

Published online: 06 September 2019

References

- Larsson E, Fredlund Fuchs P, Heldin J, Barkefors I, Bondjers C, Genove G, Arrondel C, Gerwins P, Kurschat C, Schermer B, Benzing T, Harvey SJ, Kreuger J, Lindahl P. Discovery of microvascular miRNAs using public gene expression data: miR-145 is expressed in pericytes and is a regulator of Fli1. *Genome Med.* 2009;1(11):108.
- Zhang J, Guo H, Zhang H, Wang H, Qian G, Fan X, Hoffman AR, Hu JF, Ge S. Putative tumor suppressor miR-145 inhibits colon cancer cell growth by targeting oncogene Friend leukemia virus integration 1 gene. *Cancer.* 2011;117(1):86–95.
- Starczynowski DT, Kuchenbauer F, Argiropoulos B, Sung S, Morin R, Muranyi A, Hirst M, Hogge D, Marra M, Wells RA, Buckstein R, Lam W, Humphries RK, Karsan A. Identification of miR-145 and miR-146a as mediators of the 5q-syndrome phenotype. *Nat Med.* 2010;16(1):49–58.
- Yang B, Guo H, Zhang Y, Chen L, Ying D, Dong S. MicroRNA-145 regulates chondrogenic differentiation of mesenchymal stem cells by targeting Sox9. *PLoS ONE.* 2011;6(7):e21679.

5. Fan L, Wu Q, Xing X, Wei Y, Shao Z. MicroRNA-145 targets vascular endothelial growth factor and inhibits invasion and metastasis of osteosarcoma cells. *Acta Biochim Biophys Sin.* 2012;44(5):407–14.
6. Zheng L, Pu J, Qi T, Qi M, Li D, Xiang X, Huang K, Tong Q. microRNA-145 targets v-ets erythroblastosis virus E26 oncogene homolog 1 to suppress the invasion, metastasis and angiogenesis of gastric cancer cells. *Mol Cancer Res.* 2012;11(2):182–93.
7. Gregersen LH, Jacobsen AB, Frankel LB, Wen J, Krogh A, Lund AH. MicroRNA-145 targets YES and STAT1 in colon cancer cells. *PLoS ONE.* 2010;5(1):e8836.
8. Xu Q, Liu LZ, Qian X, Chen Q, Jiang Y, Li D, Lai L, Jiang BH. MiR-145 directly targets p70S6K1 in cancer cells to inhibit tumor growth and angiogenesis. *Nucleic Acids Res.* 2012;40(2):761–74.
9. Mayorga ME, Penn MS. miR-145 is differentially regulated by TGF-beta1 and ischaemia and targets Disabled-2 expression and wnt/beta-catenin activity. *J Cell Mol Med.* 2012;16(5):1106–13.
10. Wang Z, Zhang X, Yang Z, Du H, Wu Z, Gong J, Yan J, Zheng Q. MiR-145 regulates PAK4 via the MAPK pathway and exhibits an antitumor effect in human colon cells. *Biochem Biophys Res Commun.* 2012;427(3):444–9.
11. Gotte M, Mohr C, Koo CY, Stock C, Vaske AK, Viola M, Ibrahim SA, Peddibhotla S, Teng YH, Low JY, Ebnet K, Kiesel L, Yip GW. miR-145-dependent targeting of junctional adhesion molecule A and modulation of fascin expression are associated with reduced breast cancer cell motility and invasiveness. *Oncogene.* 2010;29(50):6569–80.
12. Belleannee C, Calvo E, Thimon V, Cyr DG, Legare C, Garneau L, Sullivan R. Role of microRNAs in controlling gene expression in different segments of the human epididymis. *PLoS ONE.* 2012;7(4):e34996.
13. Kano M, Seki N, Kikkawa N, Fujimura L, Hoshino I, Akutsu Y, Chiyomaru T, Enokida H, Nakagawa M, Matsubara H. miR-145, miR-133a and miR-133b: tumor-suppressive miRNAs target FSCN1 in esophageal squamous cell carcinoma. *Int J Cancer.* 2010;127(12):2804–14.
14. Wang S, Bian C, Yang Z, Bo Y, Li J, Zeng L, Zhou H, Zhao RC. miR-145 inhibits breast cancer cell growth through RTKN. *Int J Oncol.* 2009;34(5):1461–6.
15. Cheng Y, Liu X, Yang J, Lin Y, Xu DZ, Lu Q, Deitch EA, Huo Y, Delphin ES, Zhang C. MicroRNA-145, a novel smooth muscle cell phenotypic marker and modulator, controls vascular neointimal lesion formation. *Circ Res.* 2009;105(2):158–66.
16. Chivukula RR, Mendell JT. Abate and switch: miR-145 in stem cell differentiation. *Cell.* 2009;137(4):606–8.
17. Varambally S, Cao Q, Mani RS, Shankar S, Wang X, Ateeq B, Laxman B, Cao X, Jing X, Ramnarayanan K, Brenner JC, Yu J, Kim JH, Han B, Tan P, Kumar-Sinha C, et al. Genomic loss of microRNA-101 leads to overexpression of histone methyltransferase EZH2 in cancer. *Science.* 2008;322(5908):1695–9.
18. Varnholt H, Drebber U, Schulze F, Wedemeyer I, Schirmacher P, Dienes HP, Odenthal M. MicroRNA gene expression profile of hepatitis C virus-associated hepatocellular carcinoma. *Hepatology.* 2008;47(4):1223–32.
19. Gramantieri L, Ferracin M, Fornari F, Veronese A, Sabbioni S, Liu CG, Calin GA, Giovannini C, Ferrazzi E, Grazi GL, Croce CM, Bolondi L, Negrini M. Cyclin G1 is a target of miR-122a, a microRNA frequently down-regulated in human hepatocellular carcinoma. *Cancer Res.* 2007;67(13):6092–9.
20. Bandres E, Cubedo E, Agirre X, Malumbres R, Zarate R, Ramirez N, Abajo A, Navarro A, Moreno I, Monzo M, Garcia-Foncillas J. Identification by Real-time PCR of 13 mature microRNAs differentially expressed in colorectal cancer and non-tumoral tissues. *Mol Cancer.* 2006;5:29.
21. Michael MZ, O'Connor SM, van Holst Pellekaan NG, Young GP, James RJ. Reduced accumulation of specific microRNAs in colorectal neoplasia. *Mol Cancer Res.* 2003;1(12):882–91.
22. Nam EJ, Yoon H, Kim SW, Kim H, Kim YT, Kim JH, Kim JW, Kim S. MicroRNA expression profiles in serous ovarian carcinoma. *Clin Cancer Res.* 2008;14(9):2690–5.
23. Iorio MV, Visone R, Di Leva G, Donati V, Petrocca F, Casalini P, Taccioli C, Volinia S, Liu CG, Alder H, Calin GA, Menard S, Croce CM. MicroRNA signatures in human ovarian cancer. *Cancer Res.* 2007;67(18):8699–707.
24. Schepeler T, Reinert JT, Ostenfeld MS, Christensen LL, Silahatoglu AN, Dyrskjot L, Wiuf C, Sorensen FJ, Kruhoffer M, Laurberg S, Kauppinen S, Orntoft TF, Andersen CL. Diagnostic and prognostic microRNAs in stage II colon cancer. *Cancer Res.* 2008;68(15):6416–24.
25. Yu T, Wang XY, Gong RG, Li A, Yang S, Cao YT, Wen YM, Wang CM, Yi XZ. The expression profile of microRNAs in a model of 7,12-dimethyl-benz[a]anthracene-induced oral carcinogenesis in Syrian hamster. *J Exp Clin Cancer Res.* 2009;28:64.
26. Schaefer A, Jung M, Mollenkopf HJ, Wagner I, Stephan C, Jentzmik F, Miller K, Lein M, Kristiansen G, Jung K. Diagnostic and prognostic implications of microRNA profiling in prostate carcinoma. *Int J Cancer.* 2009;126(5):1166–76.
27. Takagi T, Iio A, Nakagawa Y, Naoe T, Tanigawa N, Akao Y. Decreased expression of microRNA-143 and -145 in human gastric cancers. *Oncology.* 2009;77(1):12–21.
28. Ichimi T, Enokida H, Okuno Y, Kunimoto R, Chiyomaru T, Kawamoto K, Kawahara K, Toki K, Kawakami K, Nishiyama K, Tsujimoto G, Nakagawa M, Seki N. Identification of novel microRNA targets based on microRNA signatures in bladder cancer. *Int J Cancer.* 2009;125(2):345–52.
29. Chen HC, Chen GH, Chen YH, Liao WL, Liu CY, Chang KP, Chang YS, Chen SJ. MicroRNA deregulation and pathway alterations in nasopharyngeal carcinoma. *Br J Cancer.* 2009;100(6):1002–11.
30. Liu X, Sempere LF, Galimberti F, Freemantle SJ, Black C, Dragnev KH, Ma Y, Fiering S, Memoli V, Li H, DiRenzo J, Korc M, Cole CN, Bak M, Kauppinen S, Dmitrovsky E. Uncovering growth-suppressive MicroRNAs in lung cancer. *Clin Cancer Res.* 2009;15(4):1177–83.
31. Amaral FC, Torres N, Saggioro F, Neder L, Machado HR, Silva WA Jr, Moreira AC, Castro M. MicroRNAs differentially expressed in ACTH-secreting pituitary tumors. *J Clin Endocrinol Metab.* 2009;94(1):320–3.
32. Wang Y, Lee CG. MicroRNA and cancer—focus on apoptosis. *J Cell Mol Med.* 2009;13(1):12–23.
33. Sempere LF, Christensen M, Silahatoglu A, Bak M, Heath CV, Schwartz G, Wells V, Kauppinen S, Cole CN. Altered MicroRNA expression confined to specific epithelial cell subpopulations in breast cancer. *Cancer Res.* 2007;67(24):11612–20.
34. Zhang C. MicroRNA-145 in vascular smooth muscle cell biology: a new therapeutic target for vascular disease. *Cell Cycle.* 2009;8(21):3469–73.
35. Elia L, Quintavalle M, Zhang J, Contu R, Cossu L, Latronico MV, Peterson KL, Indolfi C, Catalucci D, Chen J, Courtneidge SA, Condorelli G. The knockout of miR-143 and -145 alters smooth muscle cell maintenance and vascular homeostasis in mice: correlates with human disease. *Cell Death Differ.* 2009;16(12):1590–8.
36. Starczynowski DT, Kuchenbauer F, Argiropoulos B, Sung S, Morin R, Muranyi A, Hirst M, Hogge D, Marra M, Wells RA, Buckstein R, Lam W, Humphries RK, Karsan A. Identification of miR-145 and miR-146a as mediators of the 5q-syndrome phenotype. *Nat Med.* 2009;16:49.
37. Bruchova H, Merkerova M, Prchal JT. Aberrant expression of microRNA in polycythemia vera. *Haematologica.* 2008;93(7):1009–16.
38. Keller A, Leidinger P, Lange J, Borries A, Schroers H, Scheffler M, Lenhof HP, Ruprecht K, Meese E. Multiple sclerosis: microRNA expression profiles accurately differentiate patients with relapsing-remitting disease from healthy controls. *PLoS ONE.* 2009;4(10):e7440.
39. Wang CJ, Zhou ZG, Wang L, Yang L, Zhou B, Gu J, Chen HY, Sun XF. Clinicopathological significance of microRNA-31, -143 and -145 expression in colorectal cancer. *Dis Markers.* 2009;26(1):27–34.
40. Pal R, Srivastava N, Chopra R, Gochhait S, Gupta P, Prakash N, Agarwal G, Bamezai RN. Investigation of DNA damage response and apoptotic gene methylation pattern in sporadic breast tumors using high throughput quantitative DNA methylation analysis technology. *Mol Cancer.* 2010;9:303.
41. Neil JR, Johnson KM, Nemenoff RA, Schiemann WP. Cox-2 inactivates Smad signaling and enhances EMT stimulated by TGF-beta through a PGE2-dependent mechanism. *Carcinogenesis.* 2008;29(11):2227–35.
42. Yata K, Bleuyard JY, Nakato R, Ralf C, Katou Y, Schwab RA, Niedzwiedz W, Shirahige K, Esashi F. BRCA2 coordinates the activities of cell-cycle kinases to promote genome stability. *Cell Rep.* 2014;7(5):1547–59.
43. Lu M, Lawrence DA, Marsters S, Acosta-Alvear D, Kimmig P, Mendez AS, Paton AW, Paton JC, Walter P, Ashkenazi A. Opposing unfolded-protein-response signals converge on death receptor 5 to control apoptosis. *Science.* 2014;345(6192):98–101.
44. Zhivotovskiy B, Kroemer G. Apoptosis and genomic instability. *Nat Rev Mol Cell Biol.* 2004;5(9):752–62.
45. Negrini S, Gorgoulis VG, Halazonetis TD. Genomic instability—an evolving hallmark of cancer. *Nat Rev Mol Cell Biol.* 2010;11(3):220–8.
46. Yang J, Weinberg RA. Epithelial–mesenchymal transition: at the crossroads of development and tumor metastasis. *Dev Cell.* 2008;14(6):818–29.

47. Tellez CS, Juri DE, Do K, Bernauer AM, Thomas CL, Damiani LA, Tessema M, Leng S, Belinsky SA. EMT and stem cell-like properties associated with miR-205 and miR-200 epigenetic silencing are early manifestations during carcinogen-induced transformation of human lung epithelial cells. *Cancer Res.* 2011;71(8):3087–97.
48. Price LS, Hajdo-Milasinovic A, Zhao J, Zwartkruis FJ, Collard JG, Bos JL. Rap1 regulates E-cadherin-mediated cell-cell adhesion. *J Biol Chem.* 2004;279(34):35127–32.
49. Bae GY, Choi SJ, Lee JS, Jo J, Lee J, Kim J, Cha HJ. Loss of E-cadherin activates EGFR-MEK/ERK signaling, which promotes invasion via the ZEB1/MMP2 axis in non-small cell lung cancer. *Oncotarget.* 2013;4(12):2512–22.
50. Hwang-Verslues WW, Chang PH, Jeng YM, Kuo WH, Chiang PH, Chang YC, Hsieh TH, Su FY, Lin LC, Abbondante S, Yang CY, Hsu HM, Yu JC, Chang KJ, Shew JY, Lee EY, et al. Loss of corepressor PER2 under hypoxia up-regulates OCT1-mediated EMT gene expression and enhances tumor malignancy. *Proc Natl Acad Sci USA.* 2013;110(30):12331–6.
51. Nam EH, Lee Y, Zhao XF, Park YK, Lee JW, Kim S. ZEB2-Sp1 cooperation induces invasion by upregulating cadherin-11 and integrin alpha5 expression. *Carcinogenesis.* 2014;35(2):302–14.
52. Chang L, Graham PH, Hao J, Ni J, Bucci J, Cozzi PJ, Kearsley JH, Li Y. Acquisition of epithelial-mesenchymal transition and cancer stem cell phenotypes is associated with activation of the PI3K/Akt/mTOR pathway in prostate cancer radioresistance. *Cell Death Dis.* 2013;4:e875.
53. John B, Enright AJ, Aravin A, Tuschl T, Sander C, Marks DS. Human MicroRNA targets. *PLoS Biol.* 2004;2(11):e363.
54. Garcia DM, Baek D, Shin C, Bell GW, Grimson A, Bartel DP. Weak seed-pairing stability and high target-site abundance decrease the proficiency of Isy-6 and other microRNAs. *Nat Struct Mol Biol.* 2011;18(10):1139–46.
55. Rehmsmeier M, Steffen P, Hochsmann M, Giegerich R. Fast and effective prediction of microRNA/target duplexes. *RNA.* 2004;10(10):1507–17.
56. Cao J, Schulte J, Knight A, Leslie NR, Zagodzdzon A, Bronson R, Manevich Y, Beeson C, Neumann CA. Prdx1 inhibits tumorigenesis via regulating PTEN/AKT activity. *EMBO J.* 2009;28(10):1505–17.

Publisher's Note

Springer Nature remains neutral with regard to jurisdictional claims in published maps and institutional affiliations.

Ready to submit your research? Choose BMC and benefit from:

- fast, convenient online submission
- thorough peer review by experienced researchers in your field
- rapid publication on acceptance
- support for research data, including large and complex data types
- gold Open Access which fosters wider collaboration and increased citations
- maximum visibility for your research: over 100M website views per year

At BMC, research is always in progress.

Learn more biomedcentral.com/submissions

